The Adsorption Behavior of Poly(acrylamide)/Poly(N-vinylpyrrolidone) Blends as Green Corrosion Inhibitors for Mg-Al Alloy: Experimental and DFT Studies

Nadia H. Helal [a] , Ghada M. Abd El-Hafeez [a] , Hassnaa H. Mohammed [a] , Moustapha E. Moustapha [b] , Zeinab R. Farag [a, *]

[a] Chemistry Department, Faculty of Science, Fayoum University, 63514 Fayoum, Egypt
[b] Department of Chemistry, College of Science and Humanities in Al-Kharj, Prince Sattam binAbdulaziz University, 11942 Al-Kharj, Saudi Arabia

A B S T R A C T

Eco-friendly organic compounds have attracted attention to be examined as corrosion inhibitors to control metallic corrosion process of pure metals and metal alloys in different media. Polymers are one of the well-known materials, which are used to inhibit metallic corrosion. The inhibition effect poly(N-vinylpyrrolidone) (PVP), poly(acrylamide) (PAM) and their blends on the corrosion behavior of magnesium alloy (Mg-10Al) in an aqueous acidic sulphate aerated unstirred solutions. Electrochemical impedance spectroscopy (EIS), potentiodynamic polarization and quantum calculations methods were used to investigate the corrosion behavior over a range of temperatures and concentrations. The data obtained from the potentiodynamic polarization method indicated that the used polymeric additives behave as a mixed-type inhibitor. The results showed that the dominant process in controlling the corrosion of the tested alloy was a charge transfer process. The corrosion inhibition efficiency was found to be 81.6% and 83% for PAM and PVP, respectively. The results showed that the adsorption of PVP and PAM on the alloy surface was found to comply with the Langmuir adsorption isotherm. A proposed mechanism was suggested to explain the inhibition action of the used polymers. Also the surface morphology was examined using atomic force microscopy AFM.

1. Introduction

In the last years the search for renewable sources of readily available materials that replaces inorganic and organic metal corrosion inhibitors CIs have continued to get more attention from scientists. Eco-friendly substances "green inhibitors" were recently tested as corrosion inhibitors because of their low-cost and are ecologically friendly, Polymers are one of well-known substances that have been used for this purpose [1-5]. Adding to the previous requirements of corrosion inhibitors, polymers were principally used due to the variety of the multiple adsorption centers in their structures and their inherent stability as well [6].

The effect of using poly (N-vinylpyrrolidone) (PVP) as corrosion inhibitor on carbon steel in an aerated alkaline corrosion medium was investigated by Al Fuhaiman et al. [7, 8]. The effect of potassium iodide and virgin Saudi clay (UC) on the effectiveness of PVP inhibition. was also tested. The outcomes of corroding solutions containing 1000 ppm PVP showed that the inhibition efficiencies ranged from 23-66% and 66-78% for the electrochemical measurements and the weight loss results respectively. The EIS measurements showed that there was a protective layer was formed as a result of PVP's adsorption.

The effectiveness of Polyacrylamide (PAM) in preventing corrosion of carbon steel in the presence and absence of Zn^{2+} was evaluated using the weight loss technique [9]. It was concluded that the protection efficiency was found to be 98%. The current work aims to investigate the inhibitory action of poly(N-vinylpyrrolidone) PVP, poly(acrylamide) PAM, and their blends on the corrosion behaviour of magnesium alloy (Mg-10Al) in an acidic environment (pH=3) containing SO_4^{2-} ions, at temperatures ranging from 25 to 60oC using potentiodynamic polarization PDP, and electrochemical impedance spectroscopy EIS techniques. Information about the adsorption of polymer could be obtained using double – layer capacitance measurements at the metal /solution interface. An attempt to correlate the adsorption and/or inhibition characteristics of PVP, PAM and their blends on magnesium alloy from acidic solutions has been made.

2. Materials and Experimental Techniques

The corrosion behavior of the alloy was evaluated using open-circuit potential and potentiodynamic measurements.

2.1. *Electrochemical Process Measurements*

A three-electrode system was used to evaluate the electrochemical performance of the Mg alloy in an acidic Na2SO4 solution. The aqueous acidic sulphate solution was prepared using analytical grade Na_2SO_4 (Sigma-Aldrich). A sensitive pH meter (BT-500 model, made in Germany) was used to monitor the pH of the solution prior to each experiment, and it was set to pH=3 by adding a few drops of H_2SO_4 solution. PVP was purchased from Sigma-Aldrich and its MW ≈40 000 g/mol. PAM was polymerized using the procedures described in the literature [10]. A 0.2mM concentration from (PAM and PVP) or their blends in the ratio [1:1, 1:3 and 3:1 (v/v)] were prepared. Volta lab potentiostat (Radiometer PGZ301) was used for the measurements. The reference was SCE and a Pt one as counter electrode. A Mg-Al rod (0.5 cm^2 surface area) was prepared in a metallurgical workshop and was used as the working electrode. Its chemical composition was presented in Table 1.

The investigated polymers were prepared with a concentration of 0.2 mM in an acidic aqueous solution of 0.5 M Na_2SO_4 and then a series dilutions were prepared. Each experiment was repeated at least three times to verify the reproducibility of the results. Electrochemical impedance spectroscopy EIS was conducted as stated in the literature [11, 12].

Table 1: Chemical composition of the Mg-Al electrode in mass %.

Sample	Al	Cu	Ni	Zn	Mn	Fe	Mg
Mg-Al	10.14	0.03	0.03	0.005	0.003	0.04	remainder

2.2. *Surface Morphology*

Non-contact mode of the atomic force microscopy (AFM) wet – SPM was used to investigate the surface morphology.

2.3. *Quantum Chemical Calculations*

Accelrys Materials Science software (MS6.0) provided the quantum calculations and optimization of the geometry of the water soluble polymers (PAM and PVP) and their blends [13, 14]. The different quantum parameters were calculated [15].

3. Results and discussion

3.1. Open-Circuit Potential Measurements

Figure 1 represented the Open- circuit potentials (OCP) of Mg-Al alloy in the presence and absence of the polymeric additive (0.2 mM) for 60 min of electrode immersion in an acidic solution of 0.5 M Na_2SO_4. In general, steady state potential was obtained within the first 25 min of immersing the electrode in the test solution. The potential became more positive with time indicating the development of a passive film on the electrode surface. It was observed that the polymeric additives shifted of the steady state potential to the positive value. The direction of the potential shift depends on the composition of the alloy as well as the origin of the inhibitor. The potential shift may be attributed to the adsorption and/or deposition of corrosion products of the inhibitor molecules on the active sites at the electrode surface.
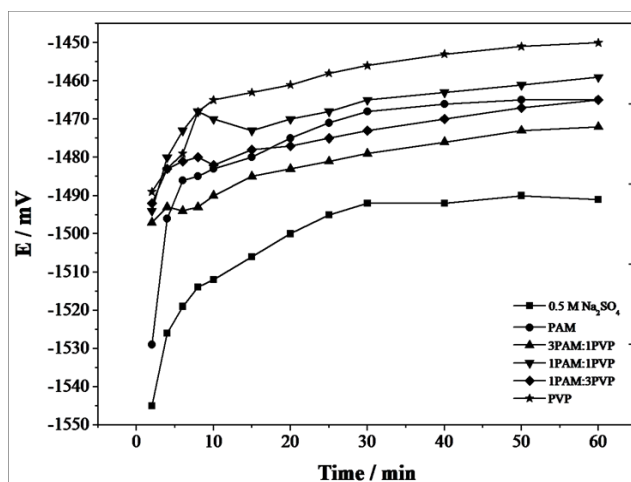
Fig. 1. Variation of the open circuit potential of Mg-Al alloy with time in an aerated stagnant acidic solution of 0.5 M Na_2SO_4 containing 0.2 mM of polymers at 25°C.

3.2. Potentiodynamic Measurements

Linear polarization and Tafel extrapolation measurements were used to evaluate the electrochemical behavior of the alloy.

3.2.1.   Effect of Polymer Structure

The effect of polymer structure on the potentiodynamic polarization curves was studied and represented in Fig.2 and Table 2. The results showed that the additives inhibited the corrosion of the alloy, and they have a trivial effect on the potentiodynamic curve shape. In addition they were slightly alter the profile of the anodic and cathodic curves without influencing the anodic and the cathodic reaction mechanism.
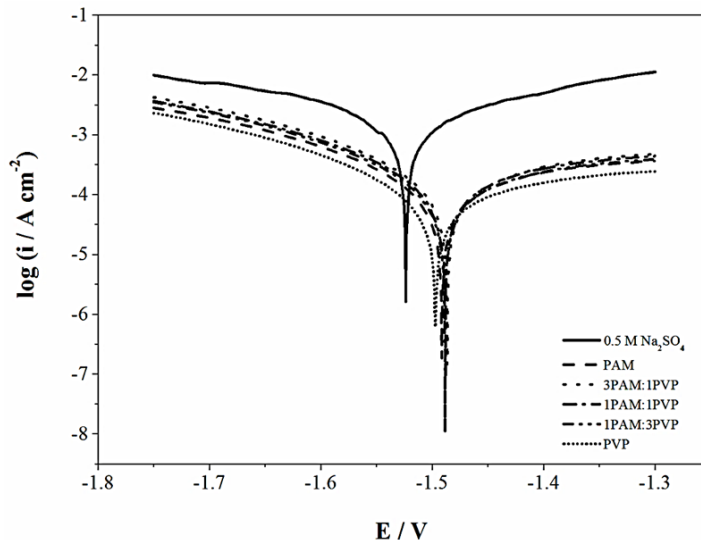

Fig. 2. Potentiodynamic polarization curves of Mg-Al alloy measured after 60 min immersion in an aerated stagnant acidic solution of 0.5 M Na_2SO_4 containing 0.2 mM of polymers at 25°C.
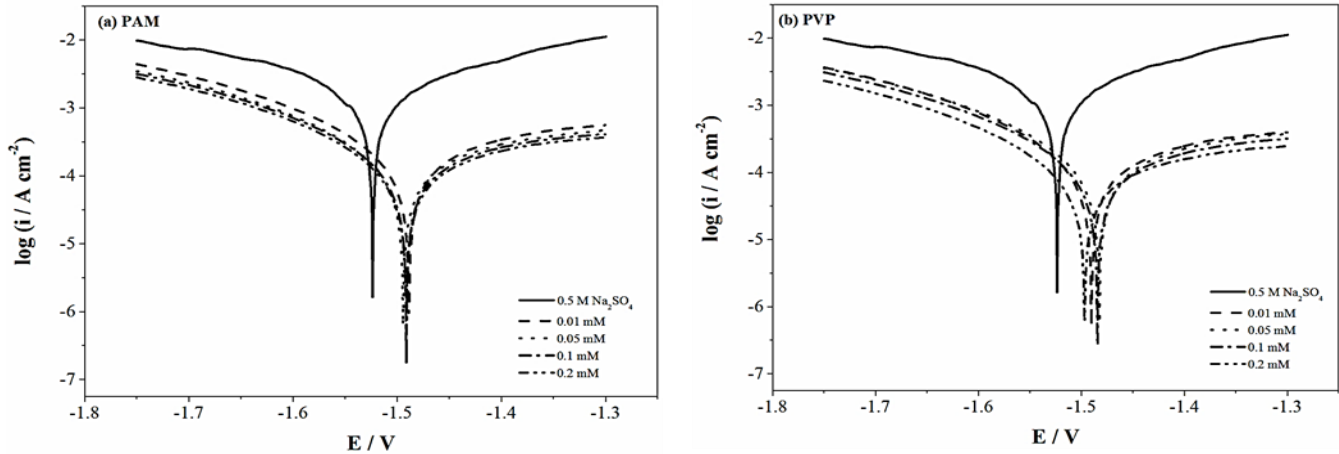
Table 2: Corrosion parameters of Mg-Al alloy measured after 60 min immersion in an aerated stagnant acidic solution of 0.5 M Na_2SO_4 containing 0.2 mM of polymers at 25°C.

inhibitors	E_{corr} (mV)	i_{corr} ($\mu A\ cm^{-2}$)	β_a (mV/dec)	β_c (mV/dec)	Rate of Corrosion ($\mu m/Y$)	η %
0.5 M Na_2SO_4	-1523.4	268.0	110.2	-99.5	6132	--
PAM	-1480.5	049.25	101.7	-76.5	1124	81.60
PAM: PVP (3:1)	-1486.3	058.93	105.4	-80.6	1344	78.01
PAM: PVP (1:1)	-1488.4	054.73	107.7	-81.4	1248	79.50
PAM: PVP (1:3)	-1488.7	051.36	107.9	-80.6	1172	80.80
PVP	-1498.9	045.46	107.9	-81.5	1037	83.03

The data showed that corrosion rate decreased in the presence of the polymeric inhibitors and the corrosion potential, Ecorr, was shifted to more positive values. From the Tafel results (Table 2), PAM and PVP were acted as a mixed-type inhibitors, which influenced the dissolution of magnesium as well as the cathodic reaction. The results showed that both PVP and PAM inhibited the corrosion of the alloy and it was found that PVP is a preferred inhibitor than PAM and blending PVA with PAM resulted in an improvement of the inhibition efficiency. The inhibition effect was due to the presence of -NH2 and -C=O groups [16], this was described in details elsewhere [17-20]. The high electro density of the N-atom stabilized the PVP molecule resulting in an enhanced surface coverage on the alloy surface, so PVP was a better inhibitor than PAM [21].

3.2.2.   Effect of Polymer Concentrations

The corrosion parameters were calculated at different concentrations of inhibitors, see Table 3 and Fig. 3. The inhibition efficiency (η) was increased upon increasing the additives concentration, and its value was found to be 81.6% and 83% for PAM and PVP, respectively.

Fig. 3. Potentiodynamic polarization curves after 60 min. immersion of the alloy in an aerated stagnant acidic solution of 0.5 M Na₂SO₄ containing different concentration of a) PAM and b) PVP at 25°C.

Table 3: Corrosion parameters of Mg-Al alloy after 60 min immersion in an aerated stagnant acidic solution of 0.5 M Na₂SO₄ containing different polymer concentrations at 25°C.

| Conc. mM	PAM				PVP			
	E_{corr} (mV)	i_{corr} (μA cm⁻²)	Corrosion rate (μm/Y)	η (%0	E_{corr} (mV)	i_{corr} (μA cm⁻²)	Corrosion rate (μm/Y)	η (%)
0.00	-1523.4	268.00	6132	--	-1523.4	268.00	6132	--
0.01	-1475.5	060.05	1370	77.6	-1490.3	050.76	1158	81.05
0.05	-1494.2	056.98	1300	78.7	-1482.5	048.92	1116	81.70
0.10	-1491.3	055.99	1277	79.1	-1484.5	047.03	1073	82.40
0.20	-1480.5	049.25	1124	81.6	-1498.9	045.46	1037	83.00

3.2.3.   *Effect of Temperature*

The effect of temperature on the inhibition efficiency (η) was studied and the current density of corrosion, icorr, was calculated. It was found the adsorption of inhibitors on the alloy surface was reduces at high temperature , which resulted in a lack in the inhibition efficiency [22]. Arrhenius equation describes the relation between the corrosion rate and temperature [23]. Fig. 4 indicated that Ea was found to be 14.43 for PAM and 14.64 kJ mol-1 for PVP,. Also, the values of Ea were found to be less than 40 kJ / mol indicating that the process was a single electron transfer process [24, 25].
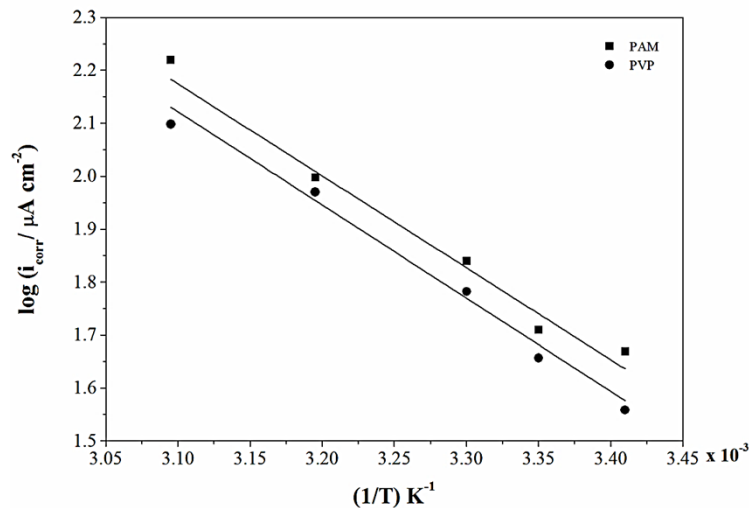
Fig. 4. Arrhenius plots of Mg-Al alloy in an aerated stagnant acidic solution of 0.5 M Na₂SO₄ containing 0.2 mM inhibitor.

3.2.4.   *The Adsorption Isotherm*

Organic compounds can control and stop the corrosion process through the adsorption of the organic inhibitors, which blocked the metal's surface [26]. Langmuir adsorption isotherm was illustrated in Figure 5, where the C was plotted versus C/θ and a straight line with an intercept of 1/K was obtained. The adsorption free energy, ΔGads, was found to be -27.7 kJ/mol for PVP -25.18 kJ/mol for PAM. Negative values indicated that the adsorption process was a spontaneous one. PAM and PVP were found to be adsorbed below -40 kJ/mol on the surface of the alloy, indicating that the adsorption is physical.
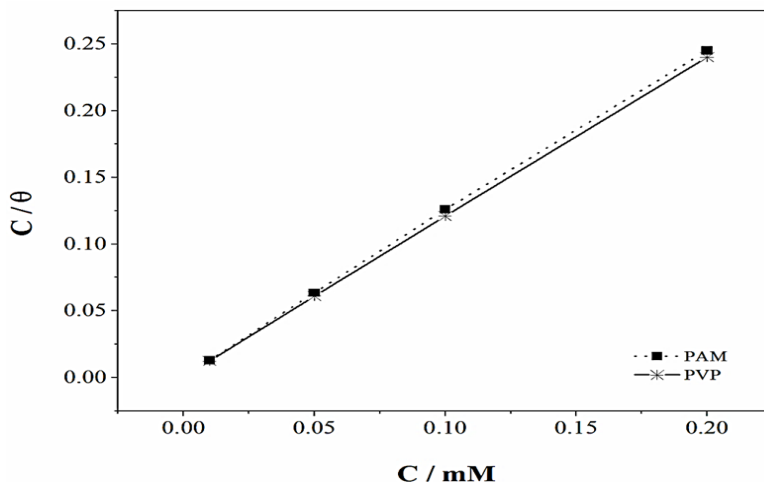
Fig. 5. Langmuir adsorption isotherm of Mg-Al alloy at different concentration of the organic inhibitors after 60 min. immersion in an aerated stagnant acidic solution of 0.5 M Na₂SO₄ at 25ᵒC.

3.3. *Electrochemical Impedance Measurements*

Electrochemical impedance techniques, EIS was used to validate the results of the potentiodynamic polarization experiments. The effect of different conditions on the corrosion process was investigated using EIS measurements.

3.3.1.   Effect of Polymer Composition

The impact of additives polymers on the corrosion of the alloy was examined. Figure 6 displays the Bode graphs of the alloy in both inhibitor-free solutions and solutions containing 0.2 mM of polymers and their various blending ratios. In the presence of polymeric additives, it was found that the electrode impedance significantly increased, indicating that the alloy surface had become less active. In addition, the phase maximum was also broadened at medium frequencies, demonstrating the existence of a protective layer [27]. An equivalent circuit was used to fit the impedance values (cf. Fig. 6 inset). The equivalent circuit parameters were calculated after 60 minutes immersion of the alloy in the working medium in the absence and presence of inhibitors as represented in Table 4. According to the findings of the EIS, the adsorption of the organic polymers led to the development of a protective layer, which caused the thickness of the electronic double layer to grow. The maximum corrosion resistance and highest $1/C_{dl}$ value were demonstrated by PVP.
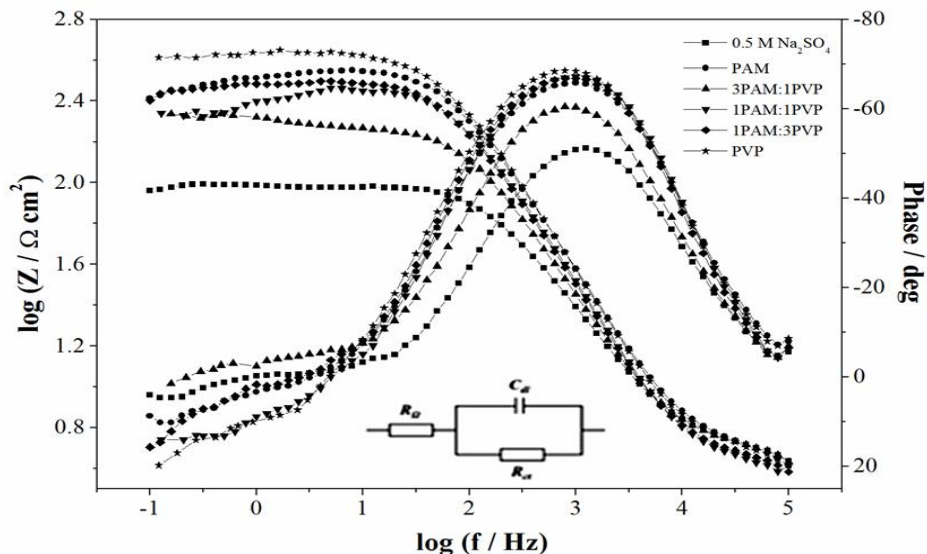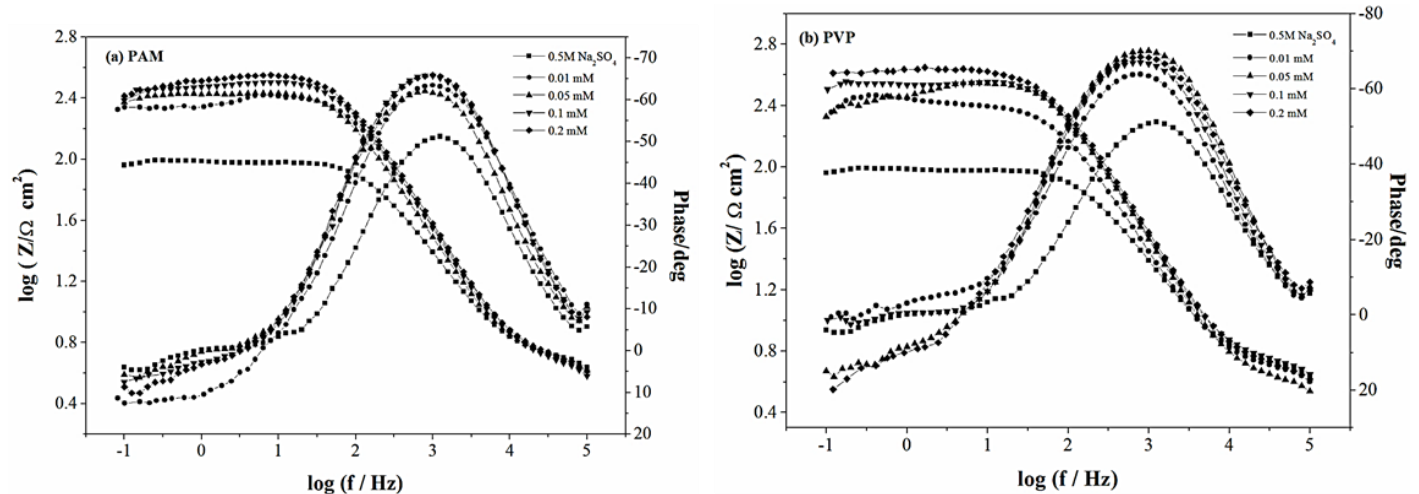

Fig. 6. Bode plots of Mg-Al alloy after 60 min. immersion in an aerated stagnant acidic solution of 0.5 M Na₂SO₄ containing 0.2 mM of polymers at 25ᵒC.

Table 4: Equivalent circuit parameters of Mg-Al alloy after 60 min. immersion in an aerated stagnant acidic solution of 0.5 M Na₂SO₄ containing 0.2 mM of polymers at 25ᵒC.

Inhibitors	R_s (Ω)	R_{ct} (Ω.cm²)	C_{dl} (µF/cm²)	α	Ƞ %
0.5 M Na₂SO₄	8.084	093.97	8.460	0.999	-
PAM	5.147	367.60	6.830	0.998	74.4
PAM: PVP (3:1)	4.969	191.80	8.293	1.000	51.0
PAM: PVP (1:1)	4.385	303.10	6.615	0.999	69.0
PAM: PVP (1:3)	4.350	329.10	7.639	1.000	71.4
PVP	4.960	429.60	5.850	0.998	78.1

3.3.2.   *Effect of Polymer Concentrations*

Fig. 7 shows Bode plots obtained from EIS analyses of Mg-Al alloy. The findings revealed a single phase maximum at the intermediate frequency, where the broadening of the maximum phase increased with increasing polymer concentration due to the formation of a protective layer on the surface.

Fig. 7. Bode plots of Mg-Al alloy after 60 min immersion in an aerated stagnant acidic solution of 0.5 M Na₂SO₄ containing different polymer concentrations at 25ᵒC a) PAM and b) PVP.

Fig. 6 as well as Tables 5 and 6 depicts the straightforward equivalent circuit model that was used to analyze the impedance data. According to the findings of these tests, a maximum film resistance was obtained at a concentration of 0.2 mM PVP. Table 5 and 6 represented the values of η and the results showed these values increased with increasing of the polymer concentration, and reached its maximum values at a concentration of 0.2 mM PVP, meaning that the PVP inhibition efficiency was better than that of PAM.

Table 5: Equivalent circuit parameters for Mg-Al alloy after 60 min immersion in an aerated stagnant acidic solution of 0.5 M Na₂SO₄ containing different concentrations of PAM at 25ᵒC.

PAM Conc. (mM)	R_s (Ω)	R_c (Ω.cm²)	C_{dl} (µF/cm²)	α	Ƞ %
0.00	8.084	093.97	8.460	0.999	-
0.01	5.132	265.00	6.005	0.998	64.5
0.05	5.373	281.10	8.945	0.997	66.6
0.10	5.282	325.40	6.162	0.996	71.1
0.20	5.147	367.60	6.839	0.998	74.4

Table 6: Equivalent circuit parameters for Mg-Al alloy after 60 min immersion in an aerated stagnant acidic solution of 0.5 M Na₂SO₄ containing different concentrations of PVP at 25ᵒC.

PVP Conc. (mM)	R_s (Ω)	R_{ct} (Ω.cm²)	C_{dl} (µF/cm²)	α	Ƞ %
0.00	8.084	093.97	8.46	0.999	-
0.01	4.891	257.30	7.79	0.999	63.5
0.05	5.047	360.10	6.98	0.995	73.9
0.10	6.210	369.70	6.80	0.995	74.6
0.20	4.960	429.60	5.85	0.998	78.1

3.4. *Surface Morphology*

The surface morphology was examined using atomic force microscopy AFM. Figure 8. showed that the morphology in the absence and in the presence of 0.2 mM PVP inhibitor. In the absence of the inhibitor, the alloy surface was rough and the surface roughness was 1.8 μm. However, the addition of 0.2 mM of PVP prevented the corrosion process and the alloy surface became smoother and the roughness was found to be 1.51 μm.
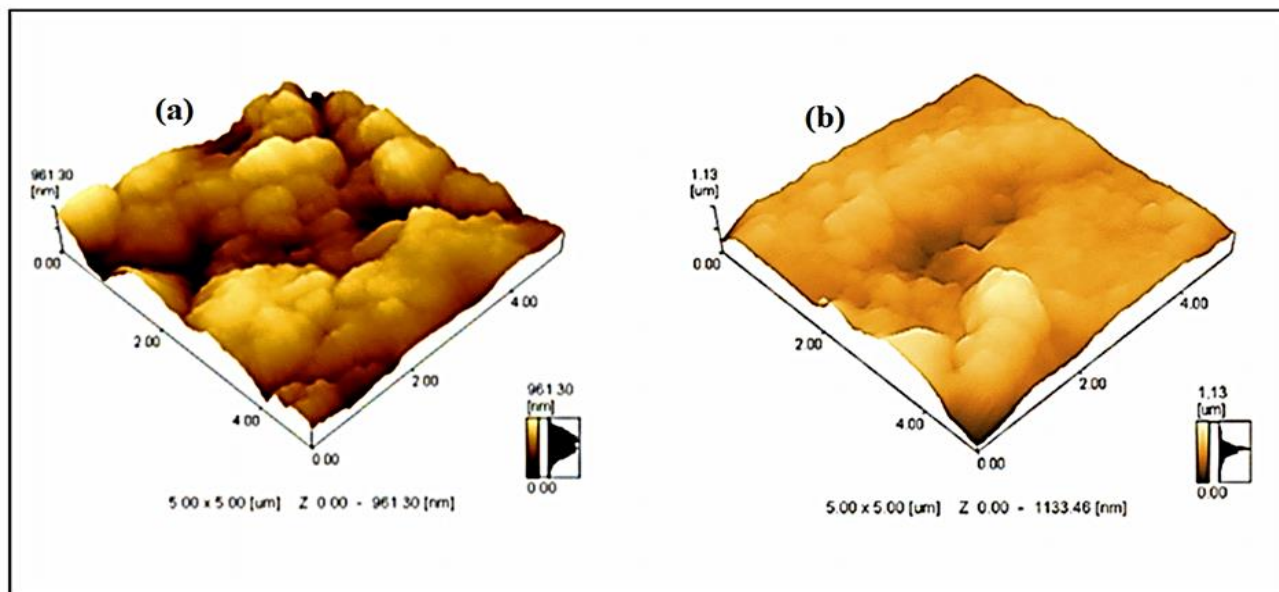

Fig. 8. AFM micrographs of the alloy surface (a) without polymer (b) in the presence of 0.2 mM PVP.

3.5. *Quantum Chemical Calculations*

3.5.1.*Computational Indices*

The most stable form of the PAM and PVP compounds, where the electron density was saturated throughout their molecules, was depicted in Figure 9. It is well known that the energy value of an inhibitor molecule's filled (EHOMO) and empty (ELUMO) orbitals, which determining its stability. Basically, low energy gab (E) values indicate good inhibition properties because the antibonding inhibitor orbital (ELUMO) will be minimised to allow electrons to be accepted from the filled Mg orbitals and the desired energy to remove the electron from the filled HOMO orbital of the inhibitor molecule will decrease, making it simpler for the Mg orbitals to accept an electron from the inhibitor molecule. The results showed that the ΔE values for PAM and PVP was 5.11262 eV and 5.071015 eV, respectively; showing higher corrosion inhibition effectiveness of PVP.
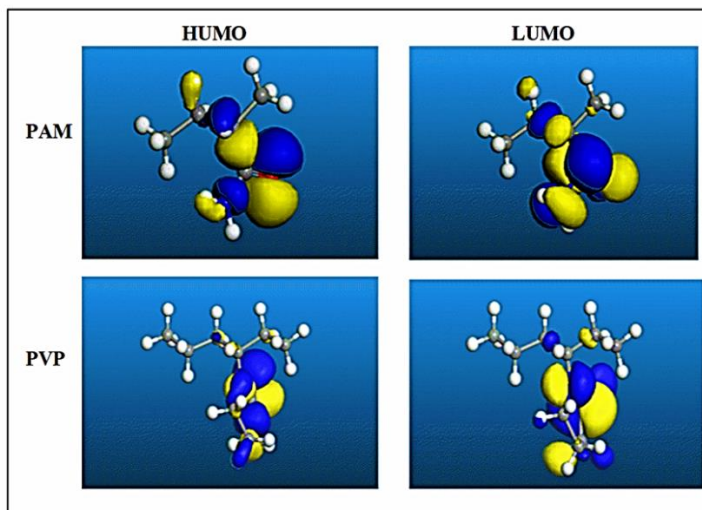

Fig. 9. The frontier molecular orbital (FMO) density distribution for the tested inhibitors PAM and PVP.

Table 7: Quantum chemical parameters of the tested polymers.

Compound	E_{HOMO} (Ha)	E_{LUMO} (Ha)	ΔE (eV)	I (eV)	A (eV)	χ (eV)	η (eV)	ΔN	μ (Debye)
PAM	-0.181725	0.006163	5.11262	4.944919	-0.1677	2.388609	2.55631	0.217	3.6353
PVP	-0.172786	0.013573	5.071015	4.70168	-0.36933	2.166172	2.535507	0.263	3.617

Because $\Delta N > 0$, electrons will transfer from inhibitors (such PAM or PVP) to the metal surface in this experiment. The PVP inhibitor has the highest electrical donation potential to the alloy surface. The ΔN value for PVP is greater than PAM indicated the higher corrosion efficency of PVP [28]. The dipole moment (μ) was another tool used to assess the probability of bond formation. It was reported that the inhibition efficiency decreased with increasing the dipole moment levels. While the lower value of (μ) may facilitate the accumulation of inhibitor molecules on the alloy surface. Also, enhancing the dipole-dipole interactions between the inhibitor molecules and the alloy surface would improve the inhibition efficacy [25, 29]. The discussed quantum parameters were in a good agreement with the theoretical assumptions.

3.5.2. Monte Carlo Simulation

Figure 10 displayed the PAM and PVP adsorption modes at top and bottom views on the Mg(110) crystal surface. The output data from the simulation method revealed that PVP's adsorption energy was larger than PAM's, indicating a more stable and powerful contact between the PVP molecule and the magnesium surface and a consequent increase in the effectiveness of the inhibition as shown in Table 8. It was noticed that Erigid values of PVP > PAM.
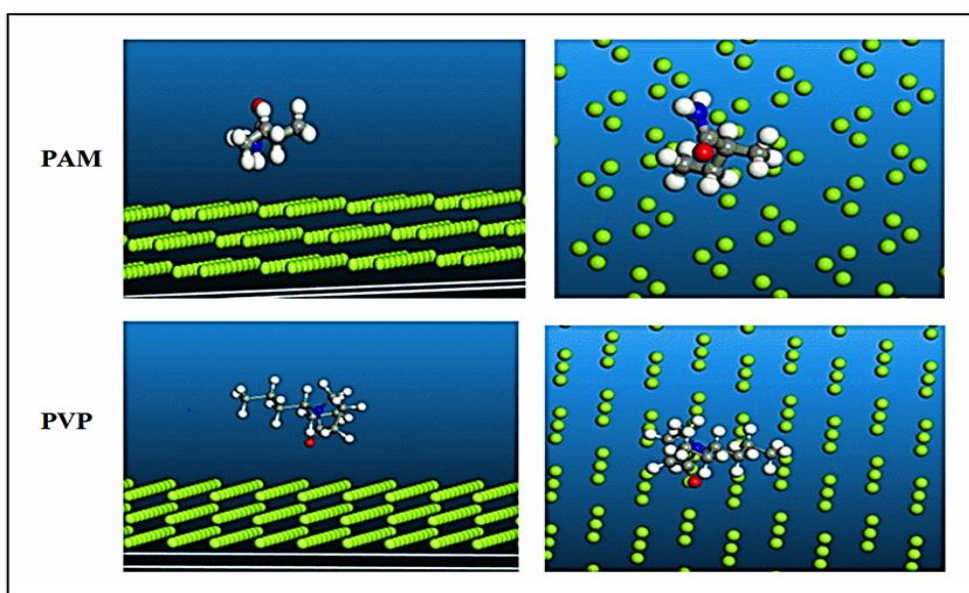
Fig. 10. Left **(**Side) and right (Top) views of the modes of adsorption of the tested polymers on the alloy surface.

Table 8: Monte Carlo simulation of the output energies

Additives Type	E_{total} (kJ/mol)	$E_{Ads.}$ (kJ/mol)	$E_{R.Ads.}$ (kJ/mol)	E_d (kJ/mol)	$dE_{ads.}/dN_i$ (kJ/mol)
PAM	00.31	- 14.90	- 04.74	- 10.15	- 14.90
PVP	14.36	- 19.55	- 06.18	- 13.37	- 19.55

4. Conclusions

The results obtained from EIS (Electrochemical Impedance Spectroscopy) and PP (Potentiodynamic Polarization) showed that PVP and PAM were effective corrosion inhibitors for the tested Mg-Al alloy in the desired working medium. For PVP and PAM, the maximum efficiencies were 83% and 81%, respectively. PVP and PAM can be categorised as a mixed type inhibitor. It could be concluded that PVP inhibits corrosion more effectively than PAM. When PVP and PAM were combined, there was evidence of compatibility since the level of inhibition efficiency increased upon increasing the percent of PVP in the blend.

Acknowledgment

Author Contributions

All authors contributed to this work. , Ghada M. Abd El-Hafeez and Hasnaa H. Mohammed   prepared the samples and completed the experimental measurements. Both N. Helal and Z. R. Farag shared writing and followed the performance of the experiments. Moustapha E. Moustapha completed the DFT calculations. Moustapha E. Moustapha with Z. R. Farag completed the paper writing, analyzing the data, and validation. Z. R. Farag followed the revision and submission of the manuscript for publication.

Declaration of Competing Interest

The authors declare that they have no known competing financial interests or personal relationships that could have appeared to influence the work reported in this paper.

References

[1] G. M. Abd El-Hafeez, M. M. El-Rabeie, A. F. Gaber, and Z. R. Farag, "Electropolymerized durable coatings deposited onto Pt-electrode as corrosion inhibitor for mild steel," *Journal of Adhesion Science and Technology,* (2021)pp. 1-19.DOI: 10.1080/01694243.2021.1963602.

[2] G. M. Abd El-Hafeez, M. M. El-Rabeie, A. F. Gaber, Z. R. Farag, and Research, "Tailored polymer coatings as corrosion inhibitor for mild steel in acid medium," *Journal of Coatings Technology,* vol. 18, no. 2(2021) pp. 581-590. https://doi.org/10.1007/s11998-020-00426-0.

[3 N. Aljeaban *et al.*, "Polymers Decorated with Functional Motifs for Mitigation of Steel Corrosion: An Overview," *International Journal of Polymer Science.* vol. 2020(2020)p. 23. doi.org/10.1155/2020/9512680.

[4] G. J. S. m. Ćirić-Marjanović, "Recent advances in polyaniline research: Polymerization mechanisms, structural aspects, properties and applications, vol. 177(2013)pp. 1-47.

[5] A. M. Elsharif, S. A. Abubshait, I. Abdulazeez, and H. A. Abubshait, "Synthesis of a new class of corrosion inhibitors derived from natural fatty acid: 13-Docosenoic acid amide derivatives for oil and gas industry," *Arabian Journal of Chemistry,* vol. 13, no. 5(2020)pp. 5363-5376,. https://doi.org/10.1016/j.arabjc.2020.03.015.

[6] S. Rajendran, S. Sridevi, N. Anthony, A. J. Amalraj, M. J. A.-C. M. Sundaravadivelu, and Materials, "Corrosion behaviour of carbon steel in polyvinyl alcohol,"vol 52(2), (2005) 102-107(6). https://doi.org/10.1108/00035590510584816.

[7] L. A. Al Juhaiman, A. A. Mustafa, W. K. Mekhamer, and Materials, "Polyvinyl pyrrolidone as a green corrosion inhibitor for carbon steel in alkaline solutions containing NaCl," *J Anti-Corrosion Methods,* vol. 60, no. 1(2013) pp. 28-36,. https://doi.org/10.1108/00035591311287429.

[8] L. A. Al Juhaiman, A. A. Mustafa, and W. K. J. I. J. E. S. Mekhamer, "Polyvinyl pyrrolidone as a green corrosion inhibitor of carbon steel in neutral solutions containing NaCl: Electrochemical and thermodynamic study," vol. 7(2012) 8578-8596,. http://www.electrochemsci.org/papers/vol7/7098578.pdf.

[9] A. Omrani, A. A. Rostami, and M. Sharifirad, "Synthesize, characterization, and corrosion inhibition of polypyrrole thin films on copper," *Journal of Macromolecular Science, Part A,* vol. 50, no. 5(2013) pp. 513-521, 10.1080/10601325.2013.780951.

[10] H.-R. Lin, "Solution polymerization of acrylamide using potassium persulfate as an initiator: kinetic studies, temperature and pH dependence," *European polymer journal,* vol. 37, no. 7(2001) pp. 1507-1510. https://doi.org/10.1016/S0014-3057(00)00261-5.

[11] M. A. Amin, "Weight loss, polarization, electrochemical impedance spectroscopy, SEM and EDX studies of the corrosion inhibition of copper in aerated NaCl solutions," *Journal of applied electrochemistry,* vol. 36, no. 2(2006) pp. 215-226. https://doi.org/10.1007/s10800-005-9055-1.

[12] E. Sherif and S.-M. Park, "Inhibition of copper corrosion in 3.0% NaCl solution by N-phenyl-1, 4-phenylenediamine," *Journal of the Electrochemical Society,* vol. 152, no. 10(2005) p. B428. https://doi.org/10.1149/1.2018254.

[13] F. E.-T. Heakal, S. Rizk, and A. Elkholy, "Characterization of newly synthesized pyrimidine derivatives for corrosion inhibition as inferred from computational chemical analysis," *Journal of Molecular Structure,* vol. 1152(2018) 328-336. https://doi.org/10.1016/j.molstruc.2017.09.079.

[14] K. Khaled, "Molecular simulation, quantum chemical calculations and electrochemical studies for inhibition of mild steel by triazoles," *Electrochimica Acta,* vol. 53, no. 9(2008)pp. 3484-3492. https://doi.org/10.1016/j.electacta.2007.12.030.

[15] N. E. Basiony, A. Elgendy, H. Nady, M. Migahed, and E. Zaki, "Adsorption characteristics and inhibition effect of two Schiff base compounds on corrosion of mild steel in 0.5 M HCl solution: experimental, DFT studies, and Monte Carlo simulation," *RSC advances,* vol. 9, no. 19(2019) 10473-10485. 10.1039/c9ra00397e.

[16] H. Ashassi-Sorkhabi, N. Ghalebsaz-Jeddi, F. Hashemzadeh, and H. Jahani, "Corrosion inhibition of carbon steel in hydrochloric acid by some polyethylene glycols," *Electrochimica acta,* vol. 51, no. 18(2006) 3848-3854. https://doi.org/10.1016/j.electacta.2005.11.002.

[17] A. Galal, N. Atta, M. Al-Hassan, and Physics, "Effect of some thiophene derivatives on the electrochemical behavior of AISI 316 austenitic stainless steel in acidic solutions containing chloride ions: I. Molecular structure and inhibition efficiency relationship," *Materials Chemistry,* vol. 89, no. 1(2005)38-48. https://doi.org/10.1016/j.matchemphys.2004.08.019.

[18] M. T. Makhlouf, S. El-Shatory, A. El-Said, and physics, "The synergistic effect of halide ions and some selected thiols as a combined corrosion inhibitor for pickling of mild steel in sulphuric acid solution," *Materials chemistry,* vol. 43, no. 1(1996). 76-82. https://doi.org/10.1016/0254-0584(95)01593-J.

[19] L. M. Vračar and D. M. Dražić, "Adsorption and corrosion inhibitive properties of some organic molecules on iron electrode in sulfuric acid," *Corrosion Science,* vol. 44, no. 8(2002) 1669-1680. https://doi.org/10.1016/S0010-938X(01)00166-4.

[20] M. Bouklah, B. Hammouti, A. Aouniti, M. Benkaddour, and A. Bouyanzer, "Synergistic effect of iodide ions on the corrosion inhibition of steel in 0.5 M H$_2$SO$_4$ by new chalcone derivatives," *Applied surface science,* vol. 252, no. 18(2006) 6236-6242. https://doi.org/10.1016/j.apsusc.2005.08.026.

[21] A. Stoyanova, G. Petkova, and S. Peyerimhoff, "Correlation between the molecular structure and the corrosion inhibiting effect of some pyrophthalone compounds," *Chemical Physics,* vol. 279, no. 1(2002)1-6. https://doi.org/10.1016/S0301-0104(02)00408-1.

[22] E. Oguzie, G. Onuoha, A. Onuchukwu, and physics, "Inhibitory mechanism of mild steel corrosion in 2 M sulphuric acid solution by methylene blue dye," *Materials chemistry,* vol. 89, no. 2-3(2005) 305-311. https://doi.org/10.1016/j.matchemphys.2004.09.004.

[23] R. G. Mortimer, *Physical chemistry*. The Benjamin/Cummings Publishing Company, Inc., Redwood City, California. 1983.

[24] F. Al-Kharafi and W. Badawy, "Inhibition of Corrosion of Al 6061, Aluminum, and an Aluminum-Copper Alloy in Chloride-Free Aqueous Media: Part 2—Behavior in Basic Solutions," *Corrosion Science,* vol. 54, no. 5,(1998)377-385. https://doi.org/10.5006/1.3284865.

[25] A. Wieckowski and E. Ghali, "On the interpretation of cyclic voltammograms of iron electrode in alkaline solution at elevated temperatures," *Electrochimica acta.* vol. 30, no. 11(1985) 1423-1431. https://doi.org/10.1016/0013-4686(85)80002-5.

[26] B. á Damaskin, O. á Petrii, and A. á Batrkov, "Adsorption of Organic Compound on Electrode," ed: Plenum, New York, 1970.

[27] W. Badawy, S. Elegamy, and K. M. Ismail, "Comparative study of tantalum and titanium passive films by electrochemical impedance spectroscopy," *British Corrosion Journal,* vol. 28, no. 2(1993)133-136, 1993. https://doi.org/10.1179/bcj.1993.28.2.133.

[28] H. Ju, Z.-P. Kai, and Y. Li, "Aminic nitrogen-bearing polydentate Schiff base compounds as corrosion inhibitors for iron in acidic media: a quantum chemical calculation," *Corrosion Science,* vol. 50, no. 3(2008) 865-871. https://doi.org/10.1016/j.corsci.2007.10.009.

[29] H. Medhashree, A. N. Shetty, and Technology, "Electrochemical corrosion study of Mg–Al–Zn–Mn alloy in aqueous ethylene glycol containing chloride ions," *Journal of Materials Research,* vol. 6, no. 1(2017)40-4z. https://doi.org/10.1016/j.jmrt.2016.04.003.